A Resonant Approach to Transformer Loss Characterization

Michael Solomentsev, Odinaka Okeke, Alex J. Hanson University of Texas at Austin 2501 Speedway, Austin, TX 78712, USA mys432@utexas.edu, odinaka@utexas.edu, ajhanson@utexas.edu

Abstract—While a transformer's inductance matrix is reasonably constant with respect to drive and frequency (up until self-resonance) and can be measured using a network analyzer, its losses are nonlinear functions of frequency and therefore difficult to characterize, especially at MHz frequencies and above. This paper presents a resonant approach to measuring a transformer's losses, including the coupled effects of both windings, at a specific operating point. We further show that, to an acceptable error, the results can be extrapolated to different operating points. The method is experimentally validated by the characterization of several transformers whose losses are confirmed by hand calculation, finite element analysis simulation, and calorimetric measurement. This work enables accurate and full characterization of transformer losses in the high frequency regime.

Index Terms—High Frequency Transformer, Core Loss, Copper Loss

I. Introduction

Many power converters rely on transformers for impedance scaling and isolation. Such transformers are among the largest and sometimes lossiest elements in a power converter. As such, it is important to properly characterize their losses which include both copper and core loss. Copper loss is regularly treated as a resistive (linear) element. In the case of an Nwinding transformer, multiple windings have various lossy interactions that must be captured by a resistance matrix [1] with N(N+1)/2 parameters. While somewhat complicated, copper loss can be measured, in principle, with small-signal measurements from instruments like network analyzers [2]-[4]. By contrast, core loss is a nonlinear phenomenon that is typically calculated using variations of the nonlinear Steinmetz equation [5], [6]. As a result, low-drive network analyzer measurements are inappropriate for capturing core loss at higher (realistic) drive levels and hence the full loss characteristics of the transformer. Large-signal loss can be measured directly from the current and voltage at the transformer ports, but these traditional IV measurements are not suitable because of the extremely high phase accuracy needed to characterize highfrequency, low-loss structures [7], [8]. As such, experimental characterization of transformer losses is often absent from academic work and industry datasheets. Frequently, finite element analysis [9]–[11] (ultimately model-based, not experimental) or thermal measurements (both slow and prone to imprecision)

This material is based upon work supported by the National Science Foundation under Grant No. DGE-1828974.

are used as stand-ins for direct electrical measurements of transformer losses.

A more suitable approach for *inductors* is to use a series resonant circuit to identify the lossy elements in a magnetic component [12]. In this approach, a high-Q capacitor is selected to resonate with the device under test. At resonance, the ratio of output to input voltage magnitudes (accurately measurable at high frequency) is equal to the quality factor of the system, which can be used to calculate the losses. Various refinements of this fundamental approach have been used to calculate the losses of magnetic cores and components [7], [13]–[16]. Most significantly, [16] extended this method to characterize the resistance matrix of air core *transformers*. This article extends this work further by applying it to transformers with non-linear loss elements, accounting for parasitics, and formalizing the method.

This work presents a generalizable method of using a series resonant circuit to fully characterize a transformer's losses, for both cored and air-core structures. We further argue that a resistance matrix description, usually only applicable to linear systems, sometimes may be used to extrapolate and predict loss at other usefully-distinct operating points with acceptable error. The full characterization approach is presented, and various contributions to error are considered and accounted for. A set of transformers are built and characterized using this method, FEA simulation, and calorimetry. This approach enables full and accurate characterization of transformers at high frequency.

II. EXPERIMENTAL METHODOLOGY FOR MEASURING TWO-PORT RESISTANCE MATRICES

We propose the following methodology for determining the resistance matrix of a two-port magnetic element. This method uses a series resonant circuit, as described in [12], to measure the effective series resistance of an inductive element. Multiple open- and short-circuit measurements can be used to determine the various parameters of the resistance matrix. We use another series resonant test to isolate the core loss present in the structure, using a modified version of the method presented in [7]. By performing this suite of tests, we identify all of the components of a transformer's (large-signal) resistance matrix and the effective core loss at a single operating point, allowing

full characterization of loss. Spreen [1] defines the loss in a two-port transformer as follows:

$$P = \frac{1}{2}R_{11}i_1i_1^* + \frac{1}{2}R_{22}i_2i_2^* + \frac{1}{2}(i_1i_2^* + i_1^*i_2)$$
 (1)

Where the R terms represent true resistance values, originating from conduction loss. Note that the original text of [1] uses R_1 to primary self-resistance, which we denote as R_{11} , instead using R_1 as the measured large-signal resistance on the primary with the secondary opened. In an effort to characterize these terms, we will evaluate the effective large-signal resistance in several different test configurations, then isolate the resistance matrix values by taking a core loss measurement. We will express this core loss as a large-signal resistance at a particular operating point: $R_{core} = 2^{P_{core}}/t_{core}^2$. In the next section, we will demonstrate that these resistances can also be used to extrapolate losses at other operating points with reasonable accuracy. For now, we note that only core loss is nonlinear. Therefore, the constant operating point can be maintained by ensuring that each test excites the same B field in the core.

First, consider driving the primary while opening the secondary winding, and resonating (by choosing C_{res}) with the primary self inductance ($L_{11} = L_m + L_{l1}$, where L_m and L_{l1} are the magnetizing and primary leakage inductance respectively, both referred to the primary). Per (1), since $i_2 = 0$, $P = \frac{1}{2}R_{11}I_1^2$ — i.e., the copper loss component measured is simply a function of R_{11} . In a transformer with core cross sectional area A_c , the peak B field, \hat{B} , can be calculated based on the measurement current I_1 :

$$V = N_1 A_c B_0 \omega = L_M I_1 \omega \tag{2}$$

$$B_0 = \frac{L_M I_1}{N_1 A_c}$$
 (3)

The total loss measured, expressed as a large-signal resistance, R_1 , is thus:

$$R_{1} = \frac{1}{I_{1}^{2}} (I_{1}^{2} R_{11} + k f^{\alpha} B_{0}^{\beta} Vol) =$$

$$R_{11} + \frac{1}{I_{1}^{2}} P_{core} = R_{11} + R_{core}$$
 (4)

We choose to express core loss as a large-signal resistance, R_{core} , that is a function of I_1 , the primary excitation current. Depending on the transformer under test, it may be more convenient to express R_{core} in terms of the secondary exciting current, and consequently refer it to the primary in further calculations.

To measure R_{22} , we repeat the same process but open-circuit the primary winding while measuring on the secondary. The peak B field will be $\hat{B} = \frac{N_2 L_M I_2}{N_1^2 A_c}$. To maintain constant B field in the core between this test and the last, $I_2 = \frac{N_1}{N_2} I_1$. The calculated large signal resistance, R_2 , will be a function of R_{22} and P_{core} , where P_{core} is the same value as in the R_1 test due to the constant B field requirement.

$$R_2 = \frac{1}{I_2^2} (I_2^2 R_{22} + k f^{\alpha} B_0^{\beta} Vol) = R_{22} + \frac{I_1^2}{I_2^2} R_{core}$$
 (5)

To identify the lossy interaction between the windings, known in linear systems as the mutual resistance, the secondary is shorted and the primary is excited. This yields an equivalent circuit as shown in Fig. 1c. We continue to assume that inductive elements will dominate over resistive ones, and that the secondary current will be in phase with the primary (which occurs when the leakage inductances are much smaller than the magnetizing inductance when all are referred to the same side of the transformer). The capacitor is now selected to resonate with the sum of the primaryreferred leakages (assuming $L_M >> (\frac{N_1}{N_2})^2 L_{l2}$). B field is now related to the magnetizing current and the secondary leakage inductance, $\hat{B} = \frac{N_1 L_{l2}}{N_2^2 A_c} I_{1s}$. Thus the magnitude of the exciting current will need to be $I_{1s} = \frac{L_m}{L_{l2}} \frac{N_2}{N_1}^2 I_1$. Assuming small secondary leakage inductance compared to magnetizing inductance, the secondary current is $-I_{1s}\frac{N_1}{N_2}$. Measuring the effective resistance of this setup yields a resistance which is a function of the core loss and all the elements of the resistance matrix. We denote the large signal resistance in this test as R_{1s} , and the copper loss component as $R_{1s,cu}$.

$$R_{1s} = \frac{1}{I_{1s}^2} (I_{1s}^2 R_{1s,cu} + k f^{\alpha} B_0^{\beta} Vol) = R_{1s,cu} + \frac{I_1^2}{I_{1s}^2} R_{core}$$
(6)

Per [1], the resistive power loss in this case will be a function of the self and mutual resistances:

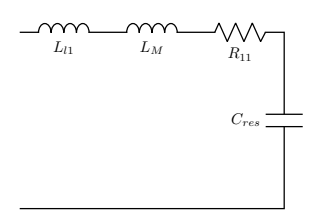
$$P_{cu} = \frac{1}{2} (R_{11} + (\frac{N_1}{N_2})^2 R_{22} - 2\frac{N_1}{N_2} R_{12}) I_{1s}^2 = \frac{1}{2} R_{1s,cu} I_1^2$$
 (7)

Thus, we can extract the mutual resistance from the measured resistance values:

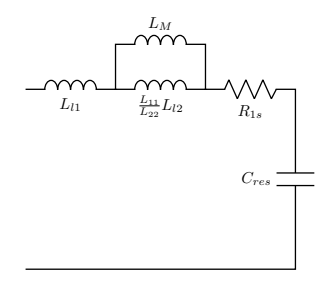
$$R_{12} = \frac{1}{2} \frac{N_2}{N_1} (R_{11} + (\frac{N_1}{N_2})^2 R_{22} - R_{1s,cu})$$
 (8)

Note that if the leakage inductance is small relative to the magnetizing inductance, the current necessary to maintain constant \hat{B} in the core may be an order of magnitude (or more) larger in the mutual resistance measurement test. Depending on the capabilities of the power amplifier used to generate the resonant signal, this may be a limiting factor for testing, particularly for cored magnetics. Section IV presents an analysis of several additional sources of error and possible solutions.

The final necessary task is to isolate core loss, such that R_{11} , R_{22} , and $R_{1s,cu}$ can be extracted from (4), (5), and (6) respectively. To measure core loss accurately, we use a modified version of the method described in [7]. Similar to the other tests described, this approach uses series resonance to isolate the relevant loss. C_{res} is chosen to resonate with a turns ratio-modified version of the magnetizing inductance. One terminal of the secondary transformer is shorted to that of the primary, and voltage is measured from the ground node to the non-shorted secondary winding. The voltage on the secondary should only depend on the magnetizing inductance, resonant capacitor, and the core loss. Since the measurement is made from the secondary winding, R_{11} does not effect the measured value. No current flows in the secondary, so R_{22} and R_{12} also do not contribute to loss. The equivalent circuit



 L_{l2} L_{22} L_{M} R_{22} C_{res}



(a) Equivalent circuit for the primary self resistance measurement

(b) Equivalent circuit for the secondary self resistance measurement

(c) Equivalent circuit for the mutual resistance measurement

Fig. 1: Equivalent circuits for each of the three measurement methods described.

for the core loss test is shown in Fig. 2.

This version eliminates the sense resistor in the original core-loss method, in favor of using the voltage on the resonant capacitor as a proxy for current. In addition, we choose not to calculate power by integrating voltage & current in the time domain, but by utilizing the peak voltage magnitudes, further reducing error.

We show the test conducted on the primary, with an open secondary winding, but it just as easily can be conducted by exciting the secondary. Just as before, the B field must be held constant, so the exciting current will simply be I_1 (the same as in the R_1 test). As described in [7], C_{res} is chosen to resonate with the magnetizing inductance adjusted by the turns ratio (the rationale for this will become apparent shortly).

$$C_{res} = \frac{1}{\omega^2 L_M} \frac{N_1}{N_2} \tag{9}$$

As a result, the core loss can be calculated from the ratio of $V_{3,pk}$ to $V_{out,pk}$, when the system is tuned to resonance (i.e. V_3 and V_{out} are 90° out of phase with each other):

$$\frac{V_{3,pk}}{V_{out,pk}} = \frac{\left|\frac{N_2}{N_1}I_1(R_{core} + j\omega L_M) + I_1\frac{1}{j\omega c_{res}}\right|}{\left|I_1\frac{1}{j\omega C_{res}}\right|} = \frac{\left|\frac{N_2}{N_1}(R_{core} + j(\omega L_M - \omega L_M))\right|}{\left|\frac{N_2}{N_1}\omega L_M\right|} = \frac{R_{core}}{\omega L_M} \quad (10)$$

With R_{core} isolated, it is now trivial to solve for R_{11} , R_{22} , $R_{1s,cu}$, and consequently R_{12} .

From these measurements, full characterization of loss in a transformer at a particular operating point can occur. For a transformer operating with primary current I_P and secondary current I_S , with expected B field B_0 , a user would identify the necessary current to achieve B_0 in the core based on (3), then conduct all of the remaining tests as described. Final loss in the transformer will then be a function of all of the calculated resistances:

$$P_{total} = P_{cu} + P_{core} = \frac{1}{2} (R_{11}I_P^2 + R_{22}I_S^2 + R_{12}(I_PI_S^* + I_P^*I_S)) + \frac{1}{2}I_P^2R_{core}$$
 (11)

We further note that in many applications, calculation of R12

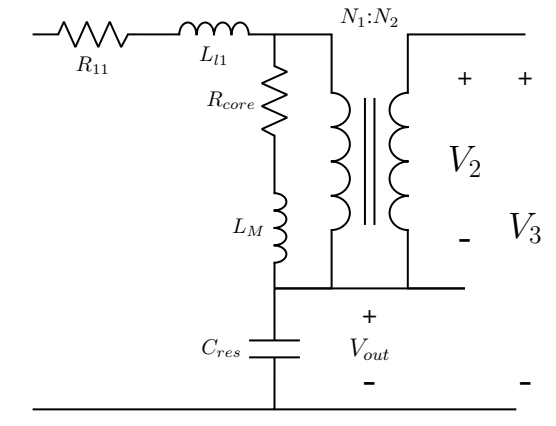


Fig. 2: Equivalent circuit for the core loss measurement method, with secondary leakage inductance and resistance omitted.

and measurement of R_{core} may not be necessary. When the transformer of interest is not designed to store energy (i.e., its primary and secondary currents will be nonzero and in phase), loss may be estimated with a high degree of accuracy by simply using the raw R_{1s} value. Similarly, in a transformer where the primary and secondary are not designed to conduct at the same time (such as a flyback transformer), loss will be dependent on R_1 and R_2 , and further measurement will not significantly increase accuracy.

III. LINEAR EXTENSION TO A RANGE OF OPERATING POINTS.

The above approach can accurately characterize transformer losses at one sinusoidal operating point (i.e., one voltage and load resistance). Naturally, these tests can be performed at multiple operating points to gain a more clear picture of transformer losses under varying conditions. In this section, we investigate the feasibility of extrapolating from a single operating point measurement to estimate the losses at other operating points.

The loss in a magnetic component (i.e. a transformer or inductor) is composed of contributions from both core and copper loss. Copper loss is typically treated as a linear phenomenon and modeled by a resistive element (although

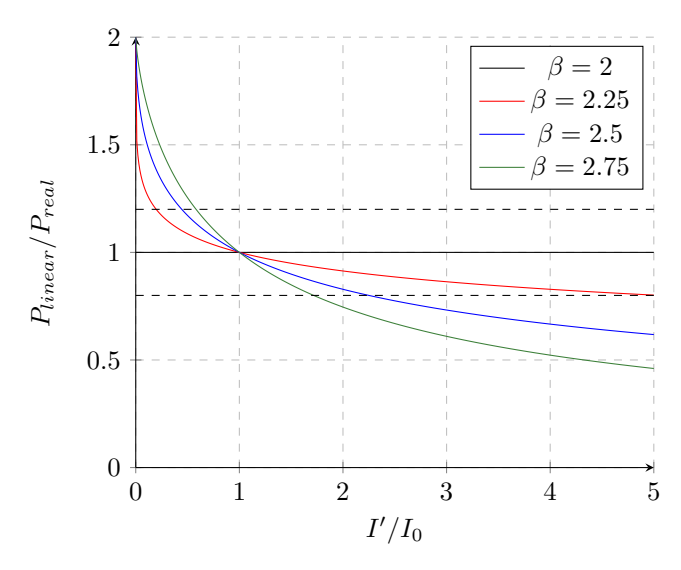


Fig. 3: Ratio between linearized and actual predicted loss in a magnetic component (assuming equal core and copper loss at the linearization point) as drive current varies. Dashed lines indicate boundaries of $\pm 20\%$ error.

copper loss does vary with temperature). Core loss, however, is non-linear, meaning it does not scale as V^2 or I^2 , and is usually modeled by some variation of the Steinmetz equation which depends on B-field, and hence current, to the power of β . Typical values of β range from 2 to 3. If drive level (i.e. the exciting current) is fixed, an equivalent large-signal core loss resistance for a certain operating point can be generated:

$$P_{core} = k f^{\alpha} \hat{B}^{\beta} Vol = k f^{\alpha} \left(\frac{LI}{NA_c}\right)^{\beta} Vol =$$

$$k f^{\alpha} \left(\frac{L}{NA_c}\right)^{\beta} Vol I^{(\beta-2)} \times I^2 = R_{core} I^2 \quad (12)$$

Thus, total loss in a magnetic structure can be expressed as simply the sum of two linear resistances:

$$P_{tot} = I^{2}(R_{cu} + R_{core}) = I^{2}R_{eff}$$
 (13)

where both R_{cu} and R_{core} are functions of frequency and drive current, i.e. they are not constant as one would expect from linear loss mechanisms.

This expression holds for constant exciting current (one experimental data point), but it is potentially useful to identify its accuracy as the component's drive current changes. Often, loss-limited magnetic components are designed to have an approximately equal division between core and copper loss in order to minimize total loss [17]. With this assumption, a ratio between the linearized and true loss can be calculated. This can be understood by considering an inductor where the core loss has been linearized around a drive current of I_0 using the equivalent large-signal resistance, and is being excited with current $I' \neq I_0$:

$$\frac{P_{linear}}{P_{real}} = \frac{I'^2 * 2R}{I'^2 (R + R \left(\frac{I'}{I_0}\right)^{\beta - 2})} = \frac{2}{1 + \left(\frac{I'}{I_0}\right)^{\beta - 2}} \quad (14)$$

This expression is plotted for various values of β in Fig. 3. Note that for a case where $\beta = 2.5$, which is typical for many materials and frequencies, the drive current can be doubled or halved relative to the experimental test point, which covers a very useful range of operation, while maintaining $\pm 20\%$ error. Furthermore, the more copper-loss-dominated a particular design is, the more accurate the linearization becomes. This is often the case for designs where large turn ratios are necessary, or potentially high current designs [18]. Also, many transformers are operated with the same voltage excitation regardless of load level. In these cases, core loss is not a function of load and treating it as a linear element incurs no inaccuracy when evaluating loss across power levels. All of this suggests that expressing loss using the largesignal linearized resistance equation is fairly robust while relying only on a single measured operating point. It may be particularly suitable for many applications where the primary interest is in estimating loss in a transformer that is typically excited around one or several operating points.

We further note that cored inductors are routinely characterized by their quality factor, $Q\left(\frac{\omega L}{R}\right)$, which implicitly linearizes the core loss present in the structure. Industry datasheets often simply provide a single Q for a part [19]. The near total ubiquity of the Q expression for inductors further indicates the utility and defensibility of the approach presented here.

IV. ERROR ANALYSIS

A. Accounting for Parasitic Capacitance

Transformers often exhibit self-resonant behavior at high frequencies due to the presence of parasitic capacitances. As the selected measurement frequency approaches the selfresonant frequency, these capacitances more substantially affect the measurements made. We attempt to quantify this effect and correct for it. While there are multiple capacitances present in the transformer under test (e.g. inter- and intrawinding capacitances), for the purposes of calculation we choose to lump these in a single parasitic capacitance C_p , as shown in Fig. 4. As the operating frequency approaches the self-resonant frequency of the test ($\omega_r = 1/\sqrt{LC_p}$), much more current will circulate in the mesh involving L, C_p , and R, causing more loss for a given net current. This is an admittedly crude model for the losses in magnetic components near selfresonance, but it has been used before to good effect [13], [14].

Note that in this analysis, the inductance and impedance are denoted as simply R and L, but they may be the relevant impedances in any of the tests depicted in Fig. 6. The core loss test, shown in Fig. 2, has a more sophisticated model for parasitic capacitances as presented in [7]. The ESR of the resonant capacitor (i.e., the one explicitly included in the measurement setup) is omitted to simplify the expression with little loss of precision. The presence of the parasitic capacitance affects both the effective resonant frequency as

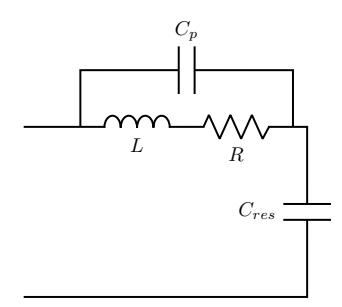


Fig. 4: Equivalent circuit showing model for parasitic capacitance in measurement setup. Note that L and R can represent the impedances of concern in any of the three tests.

well as the peak input voltage reached.

$$\omega_{res}' = \frac{jR + \sqrt{-R^2 + \frac{4L}{C_p + C_{res}}}}{2L} \approx \sqrt{\frac{1}{L(C_p + C_{res})}}$$
(15)

$$Z(\omega'_{res}) = \frac{C_p + C_{res}}{C_p C_{res}} \frac{R}{\frac{1}{C_p} - j\sqrt{\frac{1}{L(C_p + C_{res})}} R - \frac{1}{C_p + C_{res}}}$$

$$\approx \frac{(C_p + C_{res})^2}{C_{res}^2} R \quad (16)$$

The output voltage is unchanged, so the final expression for the relationship between input and output voltage at the modified resonant frequency is given by:

$$\frac{V_{out,pk}}{V_{in,pk}} = \frac{1}{R} \frac{C_{res}}{C_p + C_{res}} \frac{1}{j\omega'_{res}(C_p + C_{res})} = \frac{C_{res}}{C_p + C_{res}} \frac{\omega'_{res}L}{R} = \gamma Q \quad (17)$$

where γ denotes the parasitic capacitance correction factor. Note that to correct a resistance measurement, one must divide through by γ^2 . Refer to Fig. 5 for a plot of the correction factor versus normalized frequency. Note that when the measurement frequency is over a decade below the self resonant frequency, $.99 < \gamma < 1$. As such, correcting for parasitic capacitance only becomes necessary as the measurement frequency approaches the self-resonant frequency. This typically is a more significant source of error for the R_{11} and R_{22} tests, due to higher inductances and correspondingly, lower self-resonant frequencies. It is not recommended to use this method to characterize transformers operating above self resonance because measurements become extremely sensitive to γ .

In addition, parasitic capacitance may lead to additional circulating current to flow through the inductance under test (the loop consisting of C_p , L, and R in Fig. 4). Higher peak current would lead to higher B field in the core and a violation of the constant B field assumption outlined in Section II. As such, drive current may need to be lowered to mitigate this effect as the test frequency approaches the SRF. For a measured drive current, I_0 , the peak current in the device under

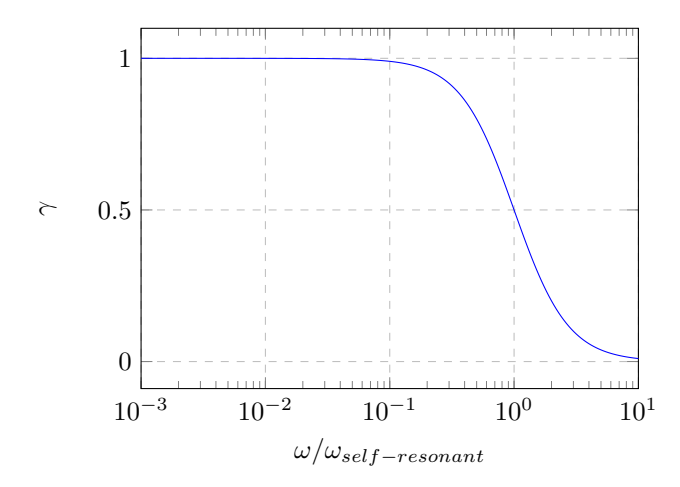


Fig. 5: Plot of parasitic capacitance correction factor γ versus frequency, normalized to the self resonant angular frequency, assuming that C_{res} is chosen simply to resonate with the inductance (and not adjusted per equation 15)

test, $I_{L,pk}$ at the new operating point can be calculated using:

$$I_{L,pk} = (1 + C_p R\omega'_{res} - \frac{C_p}{C_p + C_{res}})^{-1} I_0$$
 (18)

Note that while this expression requires knowledge of the value of resistance *a priori*, in practice the $C_pR\omega'_{res}$ term is typically insignificant. As such, a further simplification can be made to express the adjusted peak device current in terms of the correction factor:

$$I_{L,pk} \approx \frac{1}{\gamma} I_0 \tag{19}$$

This may or may not be a significant source of error depending on the magnitude of the drive current, the proximity to the self resonant frequency, and the relative dominance of nonlinear core loss phenomena in the structure. Note that (16) & (17) are not dependent on drive current, and the extracted resistance value does not need to be adjusted further. This additional expression is only relevant to peak current magnitude and resulting effects on peak B field and core loss.

We note that parasitic capacitance is most problematic when making the R_1 and R_2 measurements of the transformer, since the magnetizing impedance Z_m is very large and therefore the self-resonant frequency of the transformer is closer to the operating frequency. However, transformers designed with very high magnetizing impedance (e.g., ungapped transformers) are intended to be operated with very low magnetizing current, making the loss at the operating conditions similar to the loss measured in the R_{1s} measurement. Due to the small inductance (approximately the sum of the primary-referred leakage inductances) in this case, parasitic capacitance is not a significant factor. Thus, the measurements that have the largest difficulties with parasitic capacitance are also the least important.

B. Accounting for Large Leakage Inductance

The analysis presented in Section II assumes that in the mutual resistance test virtually all current will flow through the shorted secondary, because $L_M >> (\frac{N_1}{N_2})^2 L_{l2}$. This may not always be the case, leading to potential errors: If a more significant portion of current excites the magnetizing inductance, the B field will not be constant relative to the other tests. Moreover, the calculation of R_{12} will be inaccurate.

To maintain constant B field between tests, the exciting current must be: $I_{1s} = (1 + \frac{L_{22}L_M}{L_{11}L_{12}})I_1$. When the leakage inductance is not negligibly small compared to the magnetizing inductance, the general solution is as follows:

$$I_{sec} = -I_{1s} \frac{N_1}{N_2} \frac{L_M}{\frac{N_1}{N_2}^2 L_{l2} + L_M}$$
 (20)

$$P_{cu} = \frac{1}{2}I_{1s}^{2}(R_{1} + \left[\frac{N_{1}}{N_{2}}\frac{L_{M}}{\frac{N_{1}}{N_{2}}^{2}L_{l2} + L_{M}}\right]^{2}R_{2} - 2\frac{N_{1}}{N_{2}}\frac{L_{M}}{\frac{N_{1}}{N_{2}}^{2}L_{l2} + L_{M}}R_{12}) = \frac{1}{2}R_{1s,cu}I_{1s}^{2} \quad (21)$$

$$R_{12} = \frac{1}{2} \frac{N_2}{N_1} \frac{\frac{N_1}{N_2} L_{l2} + L_M}{L_M} (R_1 + \left[\frac{N_1}{N_2} \frac{L_M}{\frac{N_1}{N_2}^2 L_{l2} + L_M} \right]^2 R_2 - R_{1s,cu}) \quad (22)$$

C. Calculating R_{12}

Since R_{12} is calculated based on the results of multiple experimental measurements, errors have the potential to compound in its calculation $(R_{12} = \frac{1}{2} \frac{N_2}{N_1} (R_1 + (\frac{N_1}{N_2})^2 R_2 - R_{1s,cu})$. It is difficult to do a comprehensive sensitivity analysis on this calculation because error will depend not only on the relative values of each of the three measured resistances, but also the turns ratio. Qualitatively, the error in this calculation is purely a linear phenomenon. For example, in a case with a 1:1 turns ratio and $R_{11} = R_{22} = R_{meas}$, a 10% error in each value translates to a worst case error of 30% in the calculated R_{12} . This error, of course, could be less depending on the magnitudes and directions of the errors of the initial experimental measurements. In particular, if R_{12} is much smaller compared to R_{11} , R_{22} , and R_{1s} , it may be very sensitive to error in those other measurements.

V. EXPERIMENTAL VALIDATION

The proposed approach promises to accurately characterize transformer loss at a single operating point using purely electrical measurements. We validate these experimental measurements through several transformer structures, shown in Fig. 6. In each test case, the resistance matrix was extracted from finite element simulation using ANSYS Maxwell. The resistance matrix was then experimentally measured using the

method presented above. A comparison of the predictions and experimental measurements is presented in Table I.

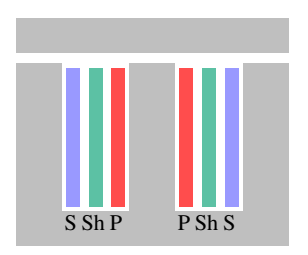
Each test was particularly designed to test a unique resistance matrix. The transformer with the small gap and shield (Fig. 6a) was designed to be core loss dominated, such that our measurements would have to distinguish between relatively small copper loss values, compared to a large core loss large-signal resistance. The transformer had a 1:1 turns ratio and was constructed with a KoolMu 90 ferrite core. Its L_{11} , L_{22} , and L_{12} were $61.37 \, \mu H$, $62.30 \, \mu H$, and $59.99 \, \mu H$ respectively.

A second test was performed using the transformer diagrammed in Fig. 6b, where we assume that there is a much larger MMF drop across the inner side of the primary winding, due to the smaller cross-sectional area (and thus higher reluctance) of the center post gap relative to the outer leg return path. As such, exciting the primary winding alone should only excite a current that flows along the inner side of that winding. Exciting the secondary, however, will excite a current that flows on the inner side of that layer and circulating currents in both the primary and shield windings. As such, it should experience significantly higher loss compared to the primary $(R_{11} \ll R_{22})$. Moreover, this structure should experience very little core loss compared to test 6a, due to its relatively large gap and small proportion of core volume. It was also constructed with a KoolMu 90 ferrite core, and had a 1:1 turns ratio. Its L_{11} , L_{22} , and L_{12} were $5.34 \,\mu\text{H}$, $5.59 \,\mu\text{H}$, and 4.92 µH respectively.

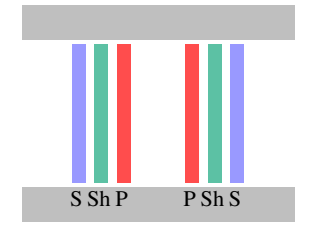
The third test was designed to operate at a higher frequency, and did not use a shield winding. It was also a 1:1 transformer, and used a PC200 RM core. Its L_{11} , L_{22} , and L_{12} were $16.66 \,\mu\text{H}$, $16.77 \,\mu\text{H}$ and $16.387 \,\mu\text{H}$ respectively.

We find that the measured resistance matrices match well with FEA simulation in all three cases, as shown in Table I. Note that ANSYS Maxwell produces a resistance matrix and a core loss value, from which we calculate a R_{core} value for comparison. It would be equivalent to express R_{core} as its equivalent power loss value. In the test cases designed to have substantial core loss (the 500 kHz transformer with a small gap and the 2 MHz transformer), the experimental core loss is extremely close to the predicted values.

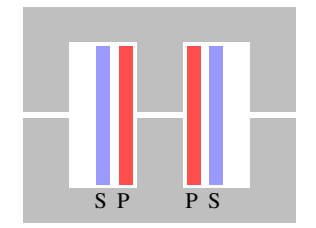
In the second test case, however, FEA simulation and experimental measurement diverge substantially – our experimental measurement of R_{core} is approximately 40x larger than FEA simulation. In this case, the B field in the core is extremely low - both simulation and hand calculation agree that it should be approximately 0.1 mT. As magnetic fields become extremely small, core loss becomes a linear phenomenon, better modeled as a true resistance (or using complex permeability) than using the non-linear Steinmetz model for loss [2]. Since the FEA solver relies on user-provided Steinmetz parameters, it categorically underestimates core loss in applications where B field is extremely low. We further validate this claim by measuring the equivalent resistance of an ungapped KoolMu 90 transformer using a E5061B Keysight Network Analyzer across various drive levels. This test confirmed that at 0.1 mT, the core is in a linear loss region, where the Steinmetz



(a) 1:1 Transformer with small gap and shield winding



(b) 1:1 Transformer with large gap and shield winding, with large center-post reluctance compared to outer-leg reluctance



(c) 1:1 Transformer with no shield winding

Fig. 6: Cross-sections of three test transformers built. Red, blue, and green rectangles represent groupings of parallel, secondary, and shielding turns respectively.

Design	Frequency	I_1	Method	R_{11}	R_{22}	R_{12}	R_{core}
1:1 w/ Shield & Small Gap	500 kHz	37 mA	FEA	.67 Ω	.87 Ω	.48 Ω	$3.63~\Omega$
			Experimental	1.11 Ω	.84 Ω	.36 Ω	$3.66~\Omega$
1:1 w/ Shield & Large Gap	500 kHz	100 mA	FEA	.23 Ω	.92 Ω	.19 Ω	$3.2\mathrm{m}\Omega$
			Experimental	.22 Ω	.88 Ω	.12 Ω	.12 Ω
1:1 w/ no Shield	2 MHz	23 mA	FEA	.45 Ω	.65 Ω	.31 Ω	.63 Ω
			Experimental	.22 Ω	.62 Ω	.15 Ω	.77 Ω

TABLE I: Predicted and experimental resistance matrices for each test case, showing strong agreement.

parameters (and thus FEA) will underestimate loss. Not only does this suggest the validity of our experimentally measured value of core loss, it serves as a powerful demonstration of the usefulness of an experimental method for transformer characterization – FEA simulation simply cannot fully model the complexities of real-world structures.

The proposed method has been additionally validated by comparison with calorimetric measurements. Calorimetry is an established method for evaluating power loss in transformers [20]–[23]. Our approach most closely resembled the procedure described in [23]. A constant volume calorimeter with no temperature feedback control was built. Measurements of the transformer temperature were made using a thermal camera. Calibration was done by putting known DC current through the structure and measuring steady-state temperature. High frequency measurements were taken while the transformer was excited at the frequency of interest by a RF power amplifier, as shown in Figure 8. Fig. 7 shows calibration and experimental data from a pot-core transformer designed to have extremely low loss when the magnetizing inductance is not excited [24]. When the secondary is shorted and the primary is driven (our R_{1s} measurement) at 1 MHz and with a drive current of 1.3 A, calorimetry found approximately 0.36 W of loss, corresponding to an effective resistance of $0.42\,\Omega$. This compares favorably with the series resonant approach, which measured 0.40Ω . Moreover, for the R_{1s} measurements for the structures shown in Figs. 6b & 6c: The proposed series resonant approach yields $1.14 \Omega \& 0.495 \Omega$, and calorimetry yields 0.9Ω & 0.46Ω respectively. Another structure, built to minimize loss when only one winding is conducting at a time [25], had its R_1 measured using both methods: the series resonant approach yielded $0.42\,\Omega$ and calorimetry yielded

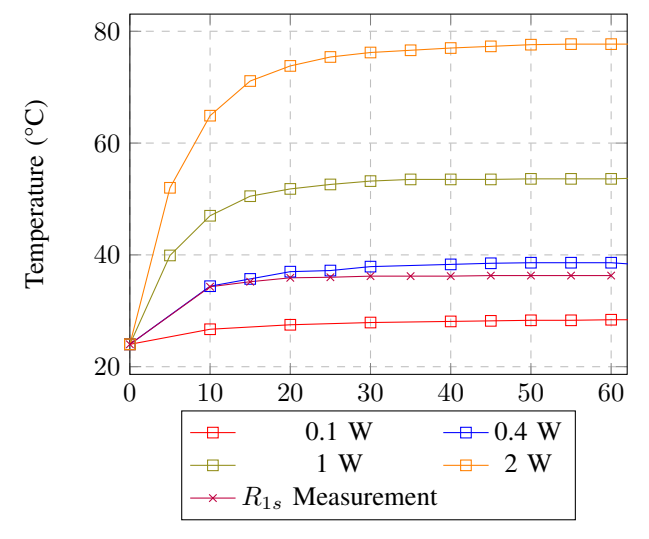


Fig. 7: Calibration and experimental calorimetry measurements for a pot-core transformer.

 $0.43\,\Omega.$ These results all further indicate the accuracy and validity of the proposed series resonant approach.

To evaluate the correction method presented in Section IV-A, the transformer depicted in Fig. 6b was tested at 3 MHz. When its primary and secondary self inductances were measured, a self resonant frequency of 11.77 MHz was measured, corresponding to an estimated 34.3 and 32.7 pF of parasitic capacitance on the primary and secondary windings respectively. When the secondary was shorted (as done in the R_{1s} measurement, the self resonant frequency was identified to be 42.57 MHz, corresponding to 12.0 pF of parasitic capacitance. The calculated correction factors for R_1 , R_2 , and R_{1s} were thus .936, .939, and .995, respectively.

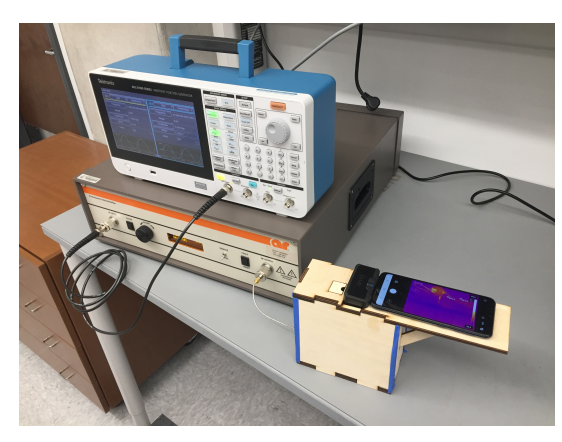


Fig. 8: Picture of the experimental high frequency calorimetry measurement setup.

 R_{core} was corrected based on the methodology suggested in [7]. The original, uncorrected values for R_{11} , R_{22} , R_{12} , and R_{core} were .29 Ω , 2.49 Ω , .01 Ω , and .91 Ω respectively. After correction, these figures changed to: .59 Ω , 3.07 Ω , .44 Ω , and .78 Ω respectively. FEA simulations resulted in predictions of .62 Ω , 2.25 Ω , .26 Ω , and .06 Ω respectively. The correction factors significantly improved the accuracy of the copper resistance measurements, compared to FEA simulation. We again note that, as described above, this test case has extremely small B field in the core, leading to inaccurate core loss predictions when using the Steinmetz based model. As such, we believe the experimental core loss value is a more accurate characterization of the transformer.

VI. CONCLUSION

This article presents a method for experimentally measuring transformer losses at one operating point. It is further argued that using the large-signal resistance matrix of a two port magnetic network can be useful to extrapolate beyond a single measured operating point with manageable error. The methodology is explained in detail and several possible sources of error are examined. The approach is tested on several test transformers and compared to theoretical calculations, FEA simulations, and calorimetric measurements – all of which show strong agreement with the presented method. This method can fully characterize the resistance matrices of magnetic components, previously only limited to simulation.

REFERENCES

- J. Spreen, "Electrical terminal representation of conductor loss in transformers," *IEEE Transactions on Power Electronics*, vol. 5, no. 4, pp. 424–429, 1990.
- [2] B. X. Foo, A. L. F. Stein, and C. R. Sullivan, "A step-by-step guide to extracting winding resistance from an impedance measurement," in 2017 IEEE Applied Power Electronics Conference and Exposition (APEC), 2017, pp. 861–867.
- [3] Y. Han, W. Eberle, and Y.-F. Liu, "A practical copper loss measurement method for the planar transformer in high-frequency switching converters," *IEEE Transactions on Industrial Electronics*, vol. 54, no. 4, pp. 2276–2287, 2007.
- [4] K. Niyomsatian, J. J. C. Gyselinck, and R. V. Sabariego, "Experimental extraction of winding resistance in litz-wire transformers—influence of winding mutual resistance," *IEEE Transactions on Power Electronics*, vol. 34, no. 7, pp. 6736–6746, 2019.

- [5] C. P. Steinmetz, "On the law of hysteresis," Transactions of the American Institute of Electrical Engineers, vol. IX, no. 1, pp. 1–64, 1892.
- [6] K. Venkatachalam, C. Sullivan, T. Abdallah, and H. Tacca, "Accurate prediction of ferrite core loss with nonsinusoidal waveforms using only steinmetz parameters," in 2002 IEEE Workshop on Computers in Power Electronics, 2002. Proceedings., 2002, pp. 36–41.
- [7] M. Mu, Q. Li, D. J. Gilham, F. C. Lee, and K. D. T. Ngo, "New core loss measurement method for high-frequency magnetic materials," *IEEE Transactions on Power Electronics*, vol. 29, no. 8, pp. 4374–4381, 2014.
- [8] L. Yi and J. Moon, "Direct in-situ measurement of magnetic loss in power electronic circuits," *IEEE Transactions on Power Electronics*, vol. 36, no. 3, pp. 3247–3257, 2021.
- [9] C. Carretero, O. Lucia, J. Acero, and J. M. Burdio, "Computational modeling of two partly coupled coils supplied by a double half-bridge resonant inverter for induction heating appliances," *IEEE Transactions on Industrial Electronics*, vol. 60, no. 8, pp. 3092–3105, 2013.
 [10] L. Keuck, F. Schafmeister, and J. Böcker, "Computer-aided design and
- [10] L. Keuck, F. Schafmeister, and J. Böcker, "Computer-aided design and optimization of an integrated transformer with distributed air gap and leakage path for an Ilc resonant converter," in 2019 IEEE Applied Power Electronics Conference and Exposition (APEC), 2019, pp. 1415–1422.
- [11] C. Feeney and N. Wang, "Ac winding loss in closed core thin film transformers accounting for two dimensional magnetic fields," in 2018 IEEE Applied Power Electronics Conference and Exposition (APEC), 2018, pp. 1794–1798.
- [12] Y. Han, G. Cheung, A. Li, C. R. Sullivan, and D. J. Perreault, "Evaluation of magnetic materials for very high frequency power applications," *IEEE Transactions on Power Electronics*, vol. 27, no. 1, pp. 425–435, 2012.
- [13] R. S. Yang, A. J. Hanson, B. A. Reese, C. R. Sullivan, and D. J. Perreault, "A low-loss inductor structure and design guidelines for high-frequency applications," *IEEE Transactions on Power Electronics*, vol. 34, no. 10, pp. 9993–10005, 2019.
- [14] R. S. Bayliss III, R. S. Yang, A. J. Hanson, C. R. Sullivan, and D. J. Perreault, "Design, implementation, and evaluation of high-efficiency high-power radio-frequency inductors," in 2021 IEEE Applied Power Electronics Conference and Exposition (APEC), 2021.
- [15] A. J. Hanson, J. A. Belk, S. Lim, C. R. Sullivan, and D. J. Perreault, "Measurements and performance factor comparisons of magnetic materials at high frequency," *IEEE Transactions on Power Electronics*, vol. 31, no. 11, pp. 7909–7925, 2016.
- [16] Z. Tong, W. D. Braun, and J. M. Rivas-Davila, "Design and fabrication of three-dimensional printed air-core transformers for high-frequency power applications," *IEEE Transactions on Power Electronics*, vol. 35, no. 8, pp. 8472–8489, 2020.
- [17] R. W. Erickson and M. Dragan, Fundamentals of power electronics. Springer, 2020.
- [18] M. K. Ranjram and D. J. Perreault, "A 380-12 v, 1-kw, 1-mhz converter using a miniaturized split-phase, fractional-turn planar transformer," *IEEE Transactions on Power Electronics*, vol. 37, no. 2, pp. 1666–1681, 2022.
- [19] Shielded High SRF Inductors 1008PS, Coilcraft Inc., 3 2020.
- [20] J. Bowman, R. Cascio, M. Sayani, and T. Wilson, "A calorimetric method for measurement of total loss in a power transformer," in PESC '91 Record 22nd Annual IEEE Power Electronics Specialists Conference, 1991, pp. 633–640.
- [21] J.-P. Keradec, "Validating the power loss model of a transformer by measurement - validation is key," *IEEE Industry Applications Magazine*, vol. 13, no. 4, pp. 42–48, 2007.
- [22] Z. Yi, H. Liu, and K. Sun, "A novel calorimetric loss measurement method for high-power high-frequency transformer based on surface temperature measurment," in 2020 4th International Conference on HVDC (HVDC), 2020, pp. 645–648.
- [23] R. Barlik, M. Nowak, P. Grzejszczak, and M. Zdanowski, "Estimation of power losses in a high-frequency planar transformer using a thermal camera," Archives of Electrical Engineering, vol. 65, 09 2016.
- [24] O. Okeke, M. Solomentsev, and A. J. Hanson, "Double-sided conduction: A loss-reduction technique for high frequency transformers," in 2022 IEEE Applied Power Electronics Conference and Exposition (APEC)), 2022.
- [25] A. Nguyen, A. Phanse, M. Solomentsev, and A. J. Hanson, "A low-leakage, low-loss magnetic transformer structure for high-frequency applications," in 2022 24th European Conference on Power Electronics and Applications (EPE'24 ECCE Europe), 2022, (Submitted).